BMES BIOMEDICAL ENGINEERING SOCIETY Check for updates

Original Article

Effect of Assistance Using a Bilateral Robotic Knee Exoskeleton on Tibiofemoral Force Using a Neuromuscular Model

Bailey J. McLain⁰, Dawit Lee⁰, Sierra C. Mulrine ¹ and Aaron J. Young^{2,3}

¹Wallace H. Coulter Department of Biomedical Engineering, Georgia Institute of Technology, 813 Ferst Dr. NW, Atlanta, GA 30332, USA; ²Woodruff School of Mechanical Engineering, Georgia Institute of Technology, Atlanta, GA, USA; and ³Institute for Robotics and Intelligent Machines, Georgia Institute of Technology, 801 Atlantic Dr. NW, Atlanta, GA 30332, USA

(Received 30 May 2021; accepted 13 March 2022; published online 27 March 2022)

Associate Editor Michael R. Torry oversaw the review of this article.

Abstract—Tibiofemoral compression forces present during locomotion can result in high stress and risk damage to the knee. Powered assistance using a knee exoskeleton may reduce the knee load by reducing the work required by the muscles. However, the exact effect of assistance on the tibiofemoral force is unknown. The goal of this study was to investigate the effect of knee extension assistance during the early stance phase on the tibiofemoral force. Nine able-bodied adults walked on an inclined treadmill with a bilateral knee exoskeleton with assistance and with no assistance. Using an EMG-informed neuromusculoskeletal model, muscle forces were estimated, then utilized to estimate the tibiofemoral contact force. Results showed a 28% reduction in the knee moment, which resulted in approximately a 15% decrease in knee extensor muscle activation and a 20% reduction in subsequent muscle force, leading to a significant 10% reduction in peak and 9% reduction in average tibiofemoral contact force during the early stance phase (p <0.05). The results indicate the tibiofemoral force is highly dependent on the knee kinetics and quadricep muscle activation due totheirinfluence on knee extensor muscle forces, the primary contributor to the knee load.

Keywords—Musculoskeletal modeling, Joint load, Biomechanics.

INTRODUCTION

The knee bears substantial mechanical loads during daily activities, especially during incline walking.^{8,21} Of these loads, the tibiofemoral force is critical due to its

Address correspondence to Bailey J. McLain, Wallace H. Coulter Department of Biomedical Engineering, Georgia Institute of Technology, 813 Ferst Dr. NW, Atlanta, GA 30332, USA. Electronic mail: bmclain3@gatech.edu

large contribution to high stress on the knee during walking, which can damage the joint.¹ Large forces present at the knee have great clinical importance and lead to subsequent injuries.⁸ For example, high-intensity joint loading can lead to osteoarthritis, the most common joint disease in the world and a leading cause of disability in the United States.^{15,27} Furthermore, individuals with pathological gait patterns, such as crouch gait, experience abnormal joint loading which can cause pain, cartilage degeneration, and bone deformities.³⁹ Thus, there are significant clinical implications in investigating ways to reduce the knee load.

Previous work by Taylor et al. has shown that tibiofemoral forces are more dependent on muscle forces than net joint reaction force.⁴⁰ Specifically, the vasti muscles are the largest contributor to the compression force in incline walking, as the increase in the knee extension moment generated during incline walking requires an increase in the knee extensor muscle force required for those walking dynamics. 11,22,35 Providing external powered assistance has the potential to assist the user by reducing the biological work performed by the muscles which may in turn reduce the tibiofemoral compression force. Previous works have investigated the efficacy of utilizing knee exoskeletons, displaying the ability to reduce the biological knee moment and knee extensor activation with assistance.^{22,32} Muscle activation and force do not always show a linear trend, because muscle forces are also dependent on fiber length and velocity.6 However, the quadricep muscles have shown a correlation between activation and

force.^{3,30} Thus, the results of these previous studies show promise that exoskeleton assistance may lead to a reduction in tibiofemoral force. However, despite a reduction in quadricep muscle activation, if co-contraction levels increase in response to the assistance, then there may be no net gain in lowering the tibiofemoral contact force. To the authors' knowledge, the exact effect of the powered assistance on the tibiofemoral force is unknown, thus further investigation is required.

To quantify the compression force, complex musculoskeletal models are frequently utilized to estimate lower limb muscle forces and joint loads during walking in both patient 18,38,39 and able-bodied populations. 1,5,35 A number of these studies use a static optimization methodology to estimate the muscle forces required to reproduce the subject's joint moment throughout the gait cycle. 16,18,39 However, this method faces the limitation that joint moments do not account for changes in muscle coactivation² or for differences in an individual's neuromuscular control system, which could be impaired.⁶ An alternative method is to use experimentally collected electromyography (EMG) data as an input to inform the neuromusculoskeletal model. 17,24,38 EMG-informed models consider the user's actual muscle activation, allowing for a more representative estimate of muscle forces.³³ This is especially critical when studying the effects of exoskeletons, as powered assistance can incite cocontraction responses unaccounted for with static optimization.¹⁴ Therefore, for this study, we utilized a hvbrid **EMG-informed** previously validated approach³⁴ with an extensively utilized model^{24,33,36} to calculate muscle forces, as it more accurately quantifies forces that consider the user's actual neuromuscular control compared to a pure static optimization.

In this paper, we present a study investigating the effect of powered assistance on the tibiofemoral compression force during incline walking for able-bodied adults, utilizing a hybrid EMG-informed neuromusculoskeletal model to estimate the muscle forces. Incline walking was selected for this study due to the walking dynamics contributing to elevated contact forces, including a 96% increase in quadricep muscle forces compared to level ground, which could potentially lead to a higher risk of soft tissue damage at the knee and the potential for the exoskeleton in offloading the biological work. The significance of the study is that it is the first to investigate the effects of exoskeleton assistance on knee loading, which has great clinical implications. The primary hypothesis is that the assistance provided at the knee during the phase in which the quadriceps are mostly active, early stance phase, will reduce the tibiofemoral contact force compared to not providing assistance. This is based on

previous works that have shown exoskeleton assistance to reduce the biological effort of the muscles surrounding the knee.²²

MATERIALS AND METHODS

Powered Bilateral Knee Exoskeleton

Hardware

This study utilized a lightweight, low-profile robotic knee exoskeleton capable of assisting the knee through powered flexion or extension assistance.²³ The output torque of the actuator was generated by a brushless DC motor (U8 LITE, T-motor, China) and a custom made single-stage 6:1 planetary gear. The peak torque of the actuator is 17.4 Nm (Table 1) which can support up to 31% of the peak biological moment of a 50th percentile weight male in the U.S.²⁹ We performed a dynamic walking test to validate the torque output capability of the device, and the root-mean-square (RMS) error between the commanded and measured torque were minimal, below 1 Nm for all walking conditions tested for this study. During unpowered walking, the RMS measured torque was 0.35 Nm meaning there is almost no resistance to the user. The motor was powered by a battery (Venom Power, USA), and the position of the motor was tracked by a 19-bit resolution encoder (Orbis, Renishaw, UK). The output torque of the actuator is transmitted to the user's knee through the thigh and shank orthotic interfaces. A force-sensitive resistor (FSR) was attached to the user's shoe to detect heel contact events. The control of the device was executed at 200 Hz using a microprocessor (myRIO 1900, National Instruments, USA). The total weight of the exoskeleton for each leg was 1.5 kg. Additionally, the subject walked while wearing a 1.3 kg control box containing electronics. The total combined weight of the bilateral exoskeleton was 4.3 kg

Controller

The powered knee exoskeleton was controlled with a biologically inspired torque controller (Fig. 1) de-

TABLE 1. Knee exoskeleton device specifications.

Max. Cont. torque (Nm)	7.2
Peak torque (Nm)	17.4
Max. speed (rad/s)	49.9
Actuator mass (kg)	0.56
Unilateral exoskeleton mass (kg)	1.5
Range of motion (°)	2 20° to 90° in flexion



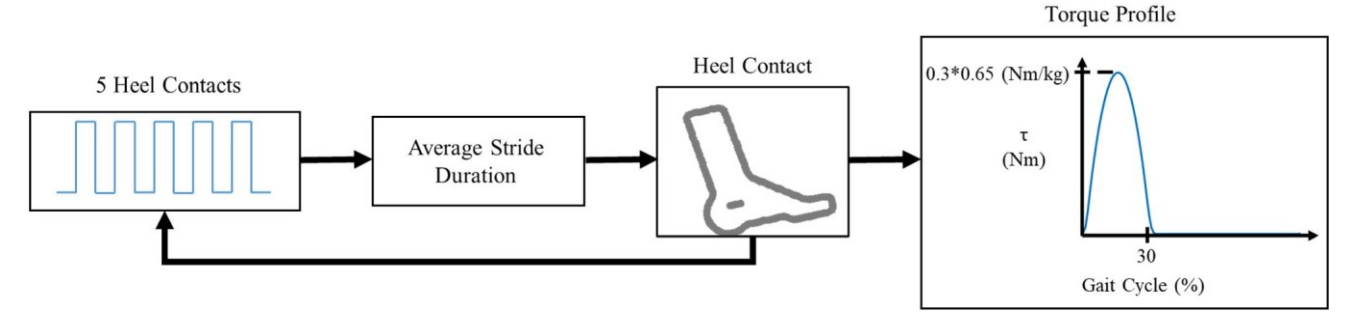


FIGURE 1. Exoskeleton control scheme. Powered extension assistance was provided for the first 30% of the gait cycle. The peak extension torque was set to be 30% of 0.65 Nm/kg, the peak biological knee moment occurring during incline walking.

signed to assist the user's knee by closely following a representative knee moment profile during the early stance phase in incline walking.¹² This is similar to biological torque controllers designed for the hip and ankle joints.^{7,19} Active assistance was provided for the first 30% of the gait cycle, called the assistance phase. The maximum torque was set to be 30% of the peak biological knee moment of an able-bodied adult occurring during incline walking, 0.65 Nm/kg.¹² This requires about 1.7 W/kg of external power consumption during the assistance mode. The user's gait phase was estimated by dividing the time since the last heel contact by the user's average stride duration. The average stride duration was computed by averaging the duration of the previous five gait cycles, updating at every heel-contact detected by the FSR. Differences in the timing between the motion capture system and the FSR were minor, with the majority of subjects displaying no difference in timing. On average, there was a delay in which the FSR was triggered 1.2% of the gait cycle later than the heel contact detected by the Bertec force plate. After the assistance phase, the commanded torque was set to 0 Nm for the remainder of the gait cycle.

Experimental Protocol

Nine able-bodied adults (5 female/4 males, mean \pm std, 21.6 \pm 3.2 years old, 173.1 \pm 7.4 cm, 67.0 \pm 5.5 kg) participated in this experiment (Fig. 2). The study was approved by the Georgia Institute of Technology Institutional Review Board. Written, informed consent was obtained from each subject before participation. Subjects walked on a treadmill at a 15% gradient incline at 1.1 m/s. Each subject participated in two visits. The first day, the exoskeleton was fitted and the subject practiced walking for 45 minutes with exoskeleton assistance to become acclimated. On the second day, the subject practiced walking for 5 minutes before the 6-minute data collection for each walking condition. The two walking conditions compared in this study

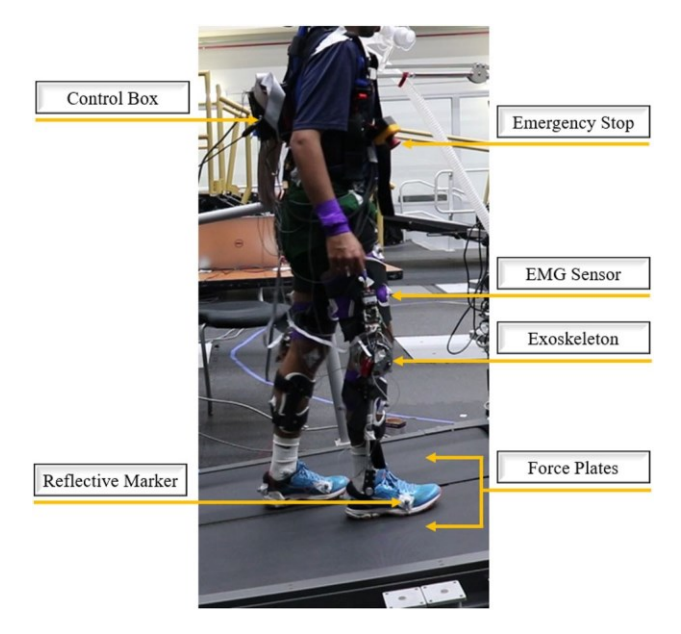


FIGURE 2. Experimental setup with callouts detailing elements of data collection and exoskeleton control. Reflective markers were used for motion capture, EMG sensors recorded muscle activation, and force plates collected ground reaction forces during walking. The control box included batteries, an EMG measurement unit, a PCB, and a microprocessor enabling control of the device.

were with assistance and without assistance (unpowered). The order of the walking conditions was randomized. After completing the exoskeleton conditions, motion capture data were also collected for a no exoskeleton condition.

Data Acquisition and Analysis

Muscle Activity

Using surface electromyography (EMG) electrodes (Biometrics Ltd., VA), the muscle activity of six major muscles around the knee on the right leg was collected at 1000 Hz. The collected muscles were: vastus lateralis (VL), rectus femoris (RF), vastus medialis (VM), biceps femoris (BF), semitendinosus (ST), and lateral



gastrocnemius (GA). These were chosen as inputs for the model because of their mechanical effect on the joint due to their large cross-sectional areas.³³ The raw EMG signals were bandpass filtered between 20 and 400 Hz, full-wave rectified, and low-pass filtered at 6 Hz to create linear envelopes. The envelopes were normalized to the maximum voluntary contraction (MVC) collected with isometric contractions targeted to each muscle group to reflect the percentage excitation level, which are the inputs to the neuromuscular model.³⁴ MVCs for the knee extensors and the hamstring muscles were collected with the knee approximating 90°. The GA MVC was completed with the knee angle at 180°.

Biomechanics

A lower-limb marker set detailed in our previous study with 28 reflective markers was utilized²² to collect motion capture data (VICON, UK) at 200 Hz. Ground reaction forces were collected from an instrumented split-belt treadmill (Bertec Corporation, Ohio) at 1000 Hz. The heel-contact was detected when the ground reaction force in the vertical direction crosses 40 N for post-processing. The hip, knee, and ankle kinematic profiles collected during the no exoskeleton condition were used to quantify the change in the kinematic patterns with exoskeleton. The kinematic deviation was computed as the average rootmean-squared error between each exoskeleton condition with respect to no exoskeleton condition.

Musculoskeletal Modeling

This study aimed to estimate the tibiofemoral contact force during walking with an exoskeleton utilizing a hybrid solution, including EMG-informed and static optimization methods to estimate the muscle forces for muscles surrounding the joint. This methodology was chosen as it enhances the representation of the musculoskeletal system compared to static optimization alone. For the simulation, a generic musculoskeletal model with 23 degrees-of-freedom and 92 musculotendon actuators to represent 76 muscles in the lower limbs and torso was utilized. 10 In this model, lower limb joint features were adopted from Delp et al. (1990), lower back anthropometry adopted from Anderson and Pandy (1999), and a planar knee model adapted from Yamaguchi and Zajac et al. (1989).4,10,42 The modeled knee is a simplified single degree of freedom model. The femoral condyles are represented as ellipses and the tibial plateau is represented as a line segment.¹⁰ The tibiofemoral contact point is specified according to data reported by Nisell et al. (1986) and is dependent on the angle of the knee.31 The muscletendon actuators for the modeled lower limbs are defined based on the anatomical landmarks on the surface of the modeled bone. 10 Optimal fiber length, pennation angle, and peak isometric forces utilized in the model are derived from Wickiewicz et al. (1983) and Friederich et al. (1990). 13,41 The model was scaled to each subject according to anthropometric measurements obtained through a static motion capture trial. Using motion capture data, joint kinematics, kinetics, and muscle-tendon unit (MTU) kinematics were calculated with OpenSim v3.3.9 The assistance torque was subtracted from the knee moment to obtain strictly the biological knee moment before use in future steps (Fig. 3). The joint kinetics, MTU kinematics, and experimentally collected EMG results were used as inputs to the Calibrated EMG-Informed Neuromus-(CEINMS).33 culoskeletal Modeling Toolbox CEINMS was used to adjust the experimental knee moment and muscle activation data to ensure agreement between the two, as well as synthesize the activations of muscles without experimentally collected data using a hybrid-mode neural solution. Of the muscles surrounding the knee, six muscles had experimentally collected activations and the other muscles were fully synthesized utilizing optimization algorithms.^{33,34} The method to adjust the joint moment, EMG data, and synthesized muscle activations used a least-squares objective function that minimized the sum of the following: the error between the estimated ðsÞ and calculated biological knee moment ð~sÞ, the error between the synthesized activation (e_i) and the experimentally collected EMG (& Þ, and the activation of synthesized muscles for muscles without experimental measurements available (Eq. 1).33

$$F_{\text{objective}}$$
 % $a \times \frac{\mathbf{P}}{\mathbf{X}^2} \frac{\mathbf{\delta} s_k}{\mathbf{p} \cdot \mathbf{S} s_k} \frac{\mathbf{F}}{\mathbf{p} \cdot \mathbf{b}} \frac{\mathbf{K}}{\mathbf{X}}$

$$\mathbf{X} \qquad e \qquad e e^2 \mathbf{p} \cdot \mathbf{c} \times \mathbf{X}$$

$$\mathbf{y} = \mathbf{y} \cdot \mathbf{m} \mathbf{T} \mathbf{u} \cdot \mathbf{s}$$

$$\mathbf{y} = \mathbf{y} \cdot \mathbf{m} \mathbf{u} \cdot \mathbf{s}$$

The weighting coefficients $\eth a; b; c$) were positive values chosen to determine the relative weighting of the error terms minimization. These coefficients were initially set based on our previous work²⁸ and manually tuned using pilot data to minimize the root mean square error (RMSE) between predicted and experimental results ($a \frac{1}{4}$ 10; 000; $b \frac{1}{4}$ 10; $c \frac{1}{4}$ 100; 000b.^{28,34}

Muscle forces $\delta F_{muscle} P$ were estimated *via* a hill-type muscle model within the CEINMS toolbox using the adjusted and synthesized activations ($e_j P$; force relative to the normalized fiber velocity $f \delta v P$, force relative to the normalized fiber length $f \delta l P$, and maximum isometric muscle fiber force based on data from the model $(F^{muscle} P)$. The Hill-type muscle model is implemented in



720 MCLAIN et al.

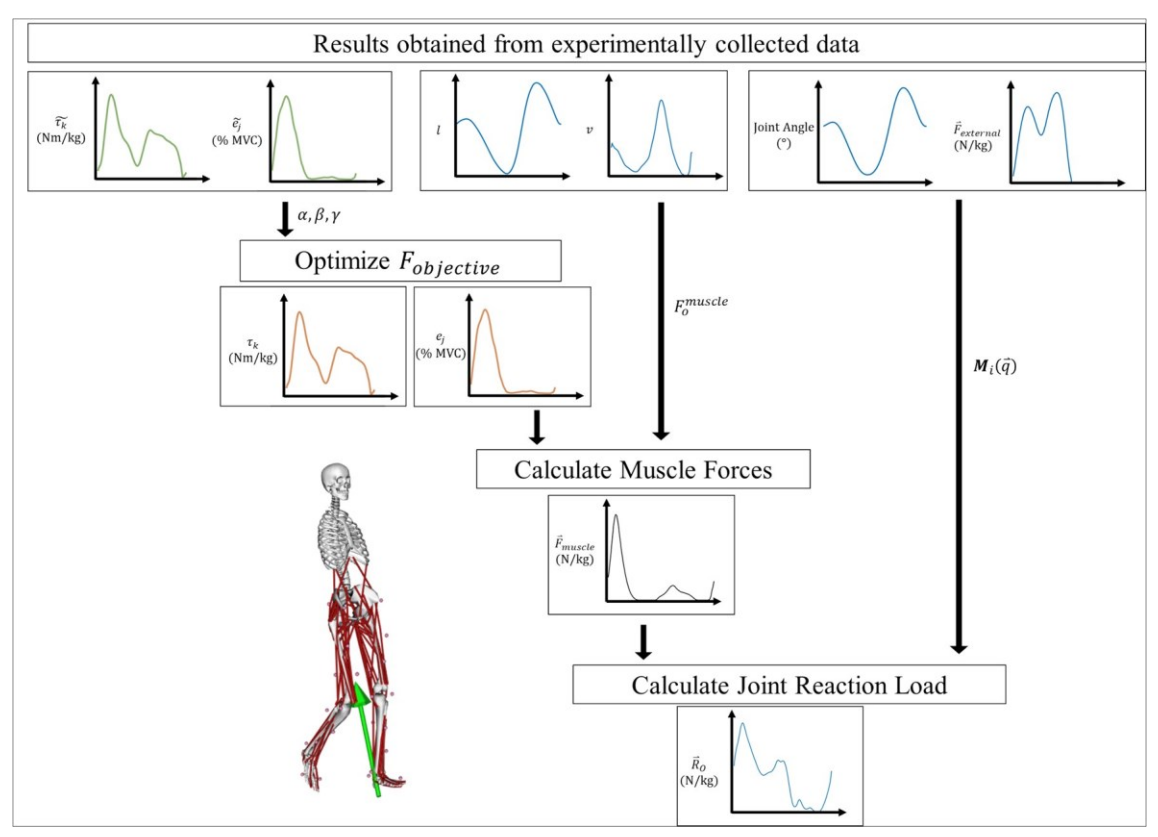


FIGURE 3. Flow diagram depicting musculoskeletal modeling. The experimentally obtained biological knee moment $\delta_s \stackrel{P}{e_k}$ and muscle activations $e_s \stackrel{Q}{e_k}$, were inputs to the objective function in CEINMS, along with the weighting coefficients $\delta a_i b_j c$). The objective function was optimized, resulting in adjusted knee moments $\delta_s \stackrel{P}{k}$ and adjusted/synthesized activations e_j for all muscles in the model. e_j , muscle fiber length, and muscle fiber velocity were then used to calculate the muscle forces $e_j \stackrel{Q}{k}$ with

a hill-type muscle model. The resultant muscle forces, joint kinematics, external forces external forces, and the mass matrix of the body ((*)) segments \mathfrak{M}_{l} were utilized to estimate the tibiofemoral contact force using Newton-Euler equation.

CEINMS in accordance with Buchanan *et al.* (2004), Lloyd and Besier (2003), and Schutte (1993) with the general form given by Eq. (2).^{6,26,33,37}

$$F_{\text{muscle}} \delta t \triangleright 4 f \delta v \triangleright X f \delta l \triangleright X e_j \delta t \triangleright X F_{o}^{\text{muscle}}$$
 $\delta 2 \triangleright$

With the hill-type muscle model, f(v) and f(l) are obtained from their respective force-velocity and force-length curves. Utilizing the MTU kinematic values calculated with OpenSim v3.3, the relative force is determined. The assisted portion of the gait cycle is characterized by eccentric contractions. This is accounted for by a derivation of the generic formula specifically for lengthening muscles as detailed by Buchanan *et al.* (2004).⁶

The estimated muscle forces $\delta F_{muscle} P$ and the joint kinematics were used as inputs for OpenSim where the tibiofemoral contact force was estimated as a point load using the Newton-Euler equation with the Joint Reaction analysis tool (Eq. 3).³⁹ The joint contact

force (R^{\triangleright}) was calculated utilizing the mass matrix for (R^{\triangleright}) the body segment \mathfrak{N}_i q, the known angular and linear accelerations of the body segment reconstructed based on the captured kinematics (a^{\bullet}_{P}) , ground reaction force data $(F_{external})$, the muscle forces applied by the musculotendon actuators $(F_{external})$, and the joint reaction load applied at the distal joint (R^{\triangleright}) .

The forces were normalized to the subject's weight and the peak and average values were compared across conditions. Tibiofemoral contact forces were analyzed during the first 30% of the gait cycle, where the ti-



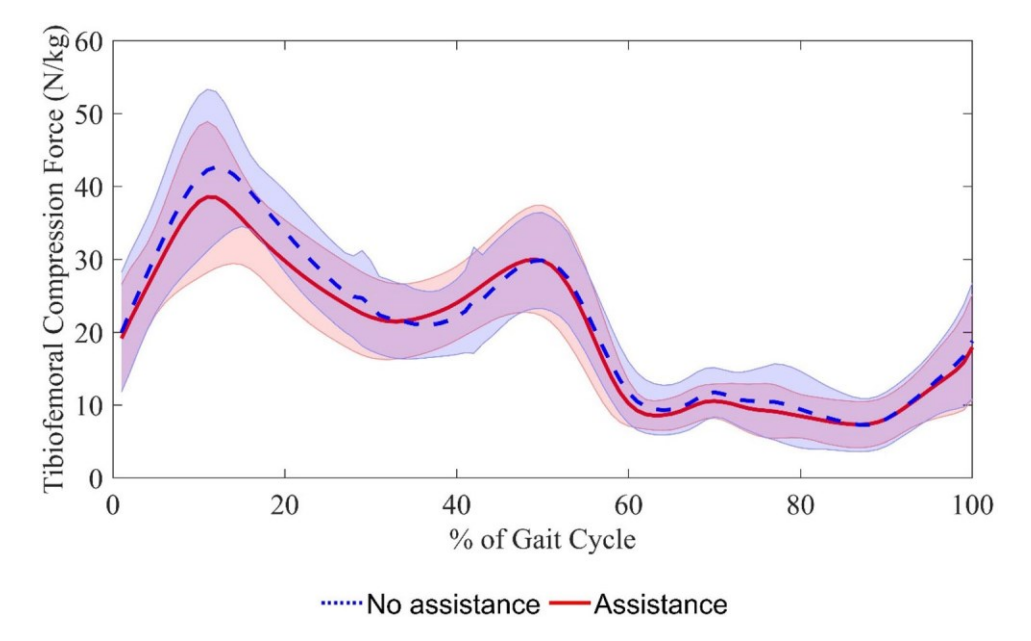


FIGURE 4. The average tibiofemoral compression force across subjects (n = 9). The solid red line denotes the assistance condition, and the dashed blue line denotes the no assistance condition. The shaded region represented $\mathbf{6}$ 1 SD.

biofemoral force is high and the active assistance was provided. For all results, the last two minutes of collected data were analyzed for the right leg.

A hybrid solution, utilizing EMG-informed and static optimized methodologies has been previously validated for the joint of interest, and has shown physiologically logical forces for the knee.³⁴ Additionally, the model used in this study has been utilized in previous works that investigate loading at the knee.^{24,36} This methodology was chosen because to the authors' knowledge, it represents the state-of-the-art non-invasive method currently utilized for joint contact force calculations.^{24,28,34,36}

For the EMG and muscle force analysis in this study, we removed one subject's ST and another subject's RF because the EMG signals had significant motion artifacts that were unable to be removed during post-processing. For those subjects, the removed activation was synthesized with the other non-collected muscles to be utilized in the joint force calculation.

Statistical Analysis

A paired t-test (p < 0.05 criterion) was utilized to test the statistical significance of the difference in outcome measures between assistance and no assistance conditions. The data is presented as the average \pm standard error of mean (SEM).

RESULTS

Tibiofemoral Compression Force

Across all subjects, the average peak tibiofemoral force was 40.5 ± 3.1 N/kg with assistance and 44.9 ± 2.8 N/kg with no assistance, displaying a significant average decrease of $10.2 \pm 2.8\%$ with assistance compared to no assistance (p < 0.01). The timing of the peak forces displayed a negligible difference between conditions. The overall average contact force during the assistance phase significantly decreased by $8.7 \pm 2.1\%$ with the assistance (p < 0.01), where the average force was 29.6 ± 1.8 N/kg with assistance and 32.4 ± 1.8 N/kg with no assistance. For the rest of the gait cycle, the tibiofemoral force showed similar trends between conditions (Fig. 4).

Muscle Forces

Of the muscles contributing to the joint load calculation, four knee extensors (VL, VI, VM, RF) displayed significant reductions in average and/or peak muscle force across the gait cycle (Table 2). The reductions primarily occurred during the assistance phase (Fig. 5). The knee flexor muscles estimated with the EMG-informed method (BF, ST, GA) displayed a non-significant increase in force, however, the knee flexor forces estimated *via* static optimization (GR, BFS, SM, SA, GAM) displayed a decrease.



TABLE 2. Percent change for average and peak muscle forces for the muscles contributing to the knee load (average 6 SEM) between assistance and no assistance.

Method	Muscle	% Change in Average Muscle Force	% Change in Peak Muscle Force
EMG-informed	Vastus lateralis (VL)	2 19.1 6 3.3	2 19.4 6 3.4
	Rectus femoris (RF)	2 16.0 6 4.2	2 21.4 6 5.3
	Vastus medialis (VM)	2 17.8 6 3.9	2 18.7 6 4.9
	Biceps femoris long head (BF)	12.9 ± 8.3	2.3 ± 5.1
	Semitendinosus (ST)	8.9 ± 4.9	1.5 ± 2.9
	Lateral gastrocnemius (GA)	0.8 ± 1.6	1.1 ± 2.2
T E S	Vastus intermedius (VI)	2 9.3 ± 3.3	2 8.3 6 2.6
	Gracilis (GR)	2 10.3 ± 6.1	2 6.4 ± 2.8
	Tensor fasciae latae (TFL)	2 13.1 ± 5.6	2 13.1 ± 7.4
	Biceps femoris short head (BFS)	2 8.8 ± 6.3	2 3.4 ± 2.2
	Semimembranosus (SM)	2 3.8 ± 10.2	2 6.9 ± 4.0
	Sartorius (SA)	2 6.8 ± 8.3	2 7.9 ± 5.5
	Medial gastrocnemius (GAM)	2 1.8 ± 4.9	2 2.9 ± 3.2

Negative values indicate a reduction with the assistance and bolded values show statistically significant differences between conditions (ρ < 0.05).

Kinematics and Kinetics

The knee displayed significant differences in joint kinematics and kinetics between conditions (Fig. 6). The peak knee flexion angle during the assistance phase significantly reduced by 3.2 ± 0.8° with the assistance (p < 0.01). The average knee extension moment during the assistance phase was significantly reduced by 27.5 \pm 8.4% compared to no assistance (p < 0.05). Additionally, the peak dorsiflexion angle significantly decreased by $1.5 \pm 0.5^{\circ}$ with assistance (p < 0.05). The hip displayed no kinematic differences and neither the hip nor ankle displayed significant kinetic changes between conditions. The average kinematic deviation over the gait cycle displayed no significant difference between the exoskeleton conditions. Furthermore, the MTU kinematics showed no significant changes between conditions, both the normalized fiber length and velocity remained consistent. The overall net power of the lower limb joints including the mechanical power from the exoskeleton to the knee has shown no difference between conditions.

Experimentally Collected Muscle Activation

The muscle activation of three knee extensors (VL, VM, and RF) displayed a statistically significant reduction in the root-mean-square average (RMSA) across the gait cycle. VL was reduced by $17.2 \pm 3.1\%$ (p < 0.004), VM was reduced by $15.4 \pm 4.0\%$ (p < 0.005), and RF was reduced by $12.6 \pm 2.8\%$ (p < 0.05). Additionally, one of the knee flexors, GA, displayed a significant increase of $8.9 \pm 3.9\%$ (p < 0.05)

between conditions. ST and BF had no significant changes in their activation between conditions (Fig. 7).

DISCUSSION

The hypothesis that the exoskeleton assistance during early stance would reduce the tibiofemoral contact force compared to the no assistance condition, exoskeleton unpowered, was supported, as the knee extension torque assistance significantly reduced the maximum (10.2% reduction) and average tibiofemoral force (8.7% reduction) during the assistance phase. The basis of the hypothesis was that extension assistance at the knee would alleviate the knee extensor muscle force required for incline walking.^{22,32} The results for the modeled muscle forces show that only the knee extensors (VL, VI, VM, and RF) displayed significant differences between conditions, primarily caused by torque assistance. Amongst the factors involved in muscle force estimation, our results showed that muscle fiber length and velocity had minimal differences between conditions. Therefore, changes in muscle activation were the primary contributor to the changes in muscle force.

The changes in muscle activation and subsequent changes in modeled muscle forces were a result of a reduction in the required kinetic effort at the knee with powered assistance. Study results show minimal changes in knee kinematics, yet a significant kinetic reduction with assistance, indicating the exoskeleton was able to offload the biological effort of the knee without drastically altering the kinematic patterns of the able-bodied subjects. Changes in kinetics have been



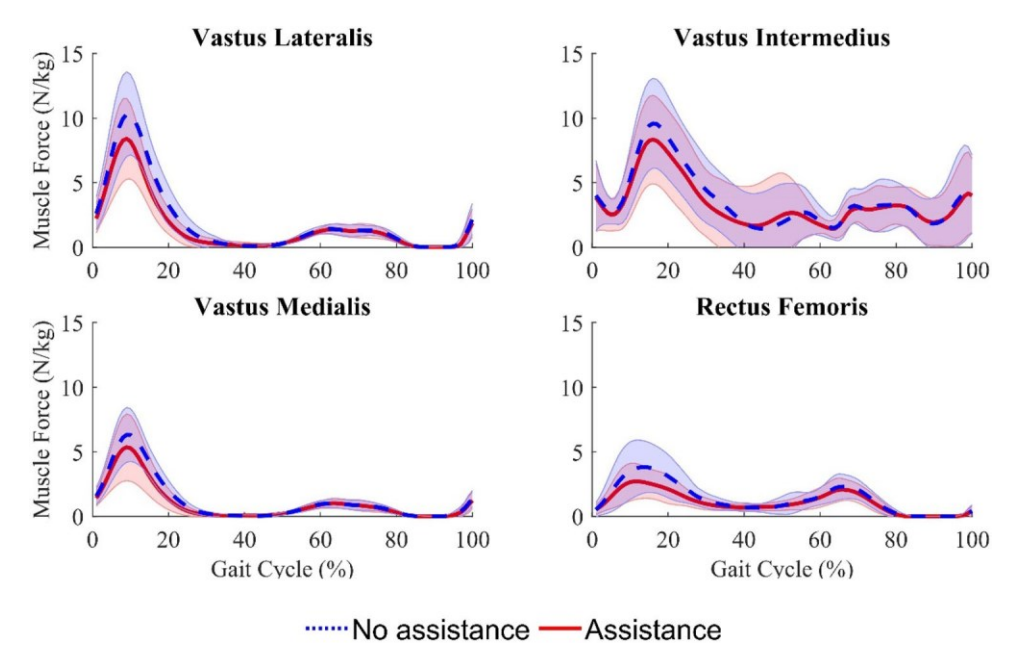


FIGURE 5. Muscle force profiles for the muscles that displayed significant changes in the muscle force with the assistance compared to the no assistance condition: VL, VI, VM, and RF. The changes in the muscles force are primarily present during the assistance phase. The shaded region represents 6 1 SD.

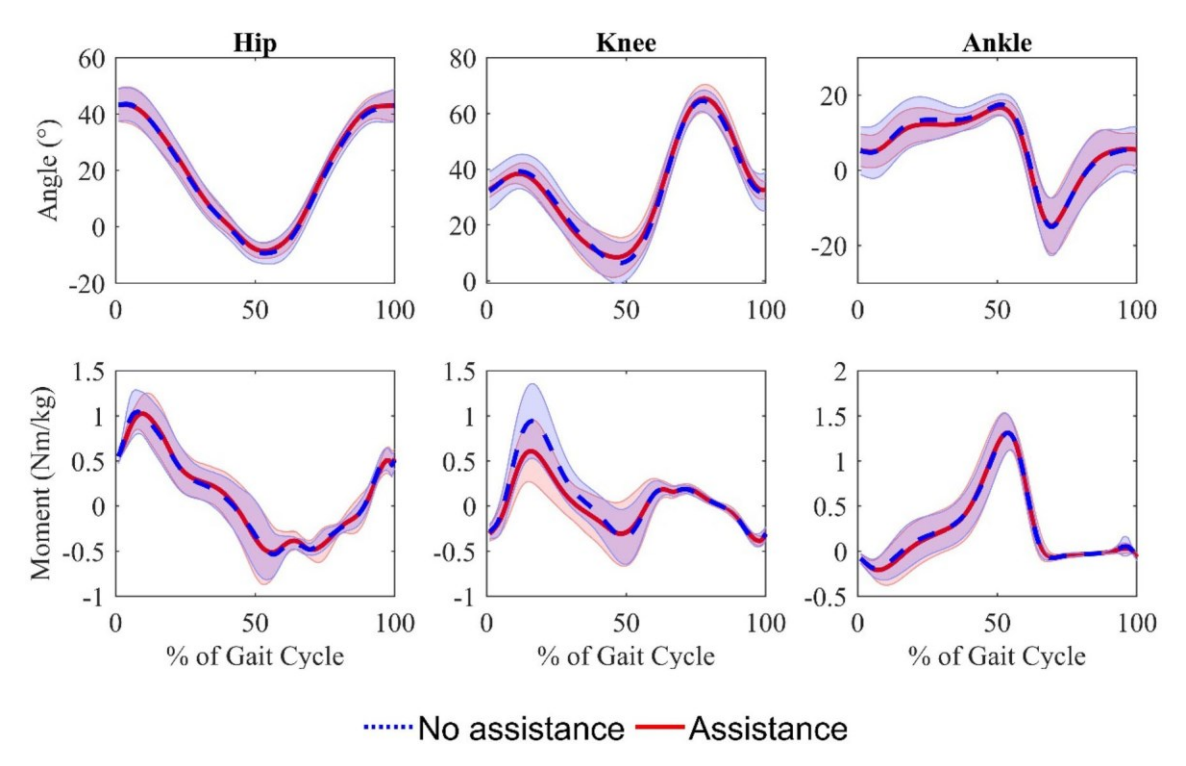


FIGURE 6. Joint kinematics and kinetics for the lower-limb joints (hip, knee, and ankle). The positive angle indicates dorsiflexion for the ankle and flexion for the hip and the knee, and the positive moment indicates plantarflexion for the ankle and extension for the hip and the knee. The red line denotes the assistance condition, and the dotted blue line denotes the no assistance condition. The shaded region represents 6 1 SD.



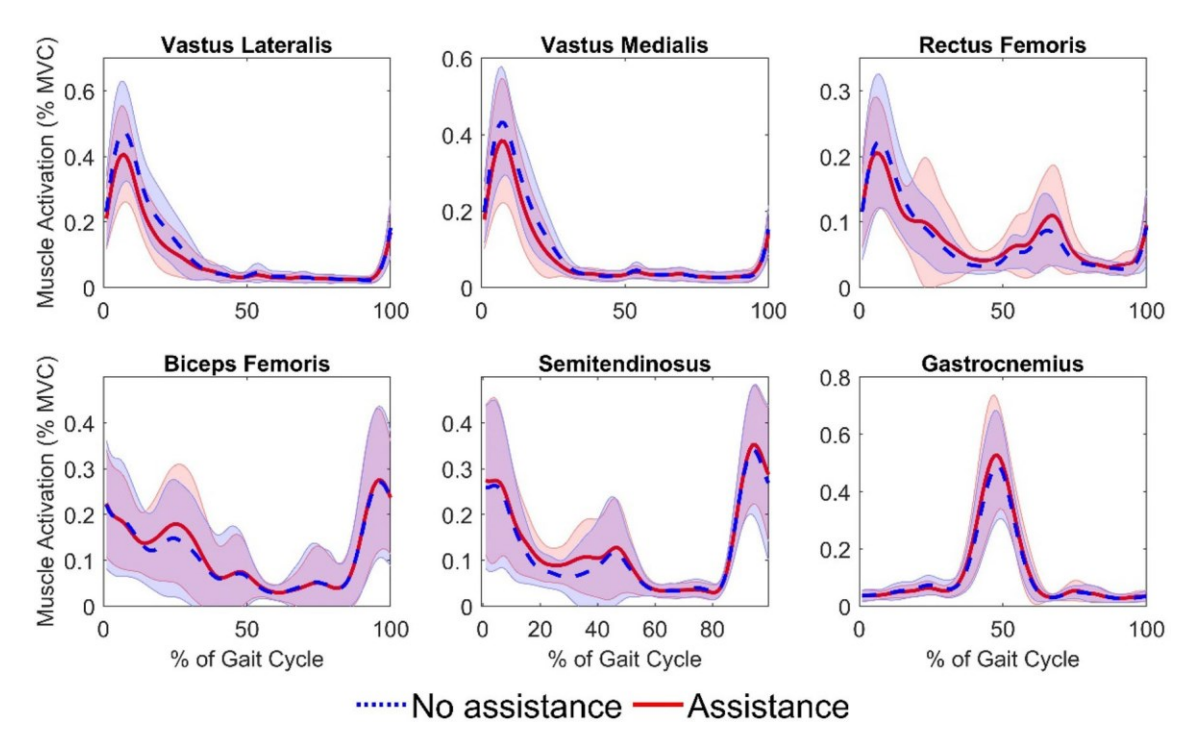


FIGURE 7. Experimentally collected electromyography results for six major muscles surrounding the knee. Significant reductions are present in early stance for the three knee extensor muscles: vastus lateralis (VL), vastus medialis (VM), and rectus femoris (RF). Additionally, a significant increase is present for the gastrocnemius (GA) muscle. The shaded region represents 6 1 SD.

of interest in previous work. DeMers et al. investigated an altered muscle coordination strategy while maintaining a kinetic outcome in a simulation. With no kinetic change, the simulated modification of vasti muscle activation was unable to change the tibiofemoral force because the required activation and force for the specified walking dynamics remained unchanged. 11 This indicates that changes in knee kinetics are vital for a reduction in muscle force. In our experimental study, the assistance significantly reduced the biological knee moment, thus the knee extensor force was reduced in agreement with the altered walking dynamics. This corresponds to the trend seen in the experimental EMG results, where the knee extensor activations significantly reduced with assistance. Thus, in our study, the tibiofemoral force reduction primarily occurred as the result of a decrease in the required kinetic effort at the knee, reducing the force demand of the knee extensor muscles.

Significant changes in muscle activation did not necessarily result in significant changes in muscle force in this study. The gastrocnemius muscle, which is both a knee flexor and plantarflexor, displayed a significant increase in activation, however, no significant difference in muscle force. This is similar to Lichtwark *et al.*'s findings showing increased muscle activation

with an increase in incline, however, no increase in muscle fascicle force. A potential reason for this is the mechanical properties of the plantarflexor muscles. *Krishnaswamy et al.* found that for the gastrocnemius, much of the MTU power comes from the tendon, not the muscle. Specifically, during late stance, the long elastic tendon provides more than 80% of the positive power generated by the MTU, reducing the mechanical work required from the muscle fascicles themselves. With this, it is indicated that muscle activations have less of an effect on changes in the muscle force for GA, 20,25 similar to our result.

There were some inconsistencies between the pure static optimization and the EMG-informed results in estimated muscle forces. Eight knee flexors were involved in the joint load calculation; five had muscle force estimations *via* static optimization without an EMG input and three had experimental EMG data to inform the estimation. The forces from the two different methods show different trends. The muscle forces estimated with the EMG-informed method displayed an increase with assistance, however, the flexor muscle forces calculated *via* pure static optimization displayed a reduction. We would expect similar responses to the assistance for the flexor muscle group, thus we expect some error in muscle forces estimated



via static optimization. Based on experimentally collected EMG results, there seems to be a co-contraction response from the antagonist muscles for some subjects during the assistance phase. The EMG-informed method accounted for this, resulting in an increase in force, however, the static optimized method that estimated force based solely on the knee moment was unable to account for the co-contraction that occurred, leading to error in the estimation.

A limitation of this study is that the results are modeled estimates of the muscle and tibiofemoral forces using a scaled generic model. Subject-specific anatomy that is not adjusted in scaling may influence specific muscle contributions to joint forces. Additionally, seven muscle forces contributing to the knee load were estimated using a pure static optimization methodology, which we expect has some error due to the inability to consider the users' actual neuromuscular control. The testing only being conducted with able-bodied individuals is also a limitation. Knee exoskeletons, like the one utilized for this study, are most likely to be applied to individuals with diminished lower limb capabilities. These patients often exhibit elevated knee extensor muscle forces and increased knee extensor moments. While the results presented here will not perfectly translate to patient groups, the muscle forces are a large contributor to the joint load for both able-bodied and patient populations. Thus, reducing the biological kinetic effort, which is demonstrated in this study, would be helpful for reducing the knee load for individuals with diminished lower limb capacities, similar to the ablebodied adults. Finally, this study has limitations in the study design. Investigating the effect of powered assistance on the tibiofemoral compression force during incline walking for able-bodied adults was the specific aim of this paper, resulting in the unpowered condition being chosen as the baseline condition. However, another interesting, and more impactful baseline for this work may be a condition without the exoskeleton to analyze the effects of the powered exoskeleton assistance compared to the subject's natural walking condition. Data from a condition without the exoskeleton was not collected for this study. Future works should investigate the effects of assistance compared to a natural condition baseline.

In conclusion, we investigated how powered exoskeleton assistance at the knee affects the tibiofermoral force utilizing a hybrid EMG-informed model. During the assistance phase, the average and peak tibiofemoral force showed significant reductions. Analyzing the muscle forces specifically, results show reductions in the quadricep muscle forces and activations caused by changes in the knee kinetics. This study shows that reducing the biological kinetic effort

required for a walking task through torque assistance can lead to offloading the required muscle forces, leading to the decreased tibiofemoral contact force. The EMG-informed neuromusculoskeletal model's incorporation of muscle coactivation displayed benefits over a purely static optimized model when analyzing exoskeleton assistance because it provided a more representative force estimate. The EMG-informed modeling and ability of the assistance to modulate knee loads discussed here could inform future works to study the effects of assistance on patient populations with large joint loads and co-contraction during ambulation, including individuals with cerebral palsy, osteoarthritis of the knee, or hemiparetic gait.

ACKNOWLEDGMENTS

This work was funded by Shriner's Hospitals for Children, NextFlex NMMI Grant, NSF NRI Award #1830498, Georgia Tech Petit Research Scholar Program, and The Imlay Foundation.

CONFLICT OF INTEREST

There is no conflict of interest reported by the authors.

REFERENCES

- ¹Alexander, N., and H. Schwameder. Effect of sloped walking on lower limb muscle forces. *Gait & Posture*. 47:62–67, 2016.
- ²Alexander, N., and H. Schwameder. Lower limb joint forces during walking on the level and slopes at different inclinations. *Gait & Posture*. 45:137–142, 2016.
- ³Alkner, B. A., P. A. Tesch, and H. E. Berg. Quadriceps EMG/force relationship in knee extension and leg press. *Med. Sci. Sports Exerc.* 32(2):459–463, 2000.
- ⁴Anderson, F., and M. Pandy. A dynamic optimization solution for vertical jumping in three dimensions. *Comput. Methods Biomech. Biomed. Eng.* 2:201–231, 1999.
- ⁵Arnold, E. M., S. R. Hamner, A. Seth, M. Millard, and S. L. Delp. How muscle fiber lengths and velocities affect muscle force generation as humans walk and run at different speeds. *J. Exp. Biol.* 216:2150, 2013.
- ⁶Buchanan, T. S., D. G. Lloyd, K. Manal, and T. F. Besier. Neuromusculoskeletal modeling: estimation of muscle forces and joint moments and movements from measurements of neural command. *J. Appl. Biomech.* 20:367–395, 2004
- ⁷Cain, S. M., K. E. Gordon, and D. P. Ferris. Locomotor adaptation to a powered ankle-foot orthosis depends on control method. *J. NeuroEng. Rehabil.* 4:48, 2007.
- ⁸D'Lima, D. D., B. J. Fregly, S. Patil, N. Steklov, and C. W. Colwell Jr. Knee joint forces: prediction, measurement,



and significance. Proc. Inst. Mech. Eng. Part H. 226:95–102, 2012.

- ⁹Delp, S. L., F. C. Anderson, A. S. Arnold, P. Loan, A. Habib, C. T. John, E. Guendelman, and D. G. Thelen. OpenSim: open-source software to create and analyze dynamic simulations of movement. *IEEE Trans. Biomed. Eng.* 54:1940–1950, 2007.
- ¹⁰Delp, S. L., J. P. Loan, M. G. Hoy, F. E. Zajac, E. L. Topp, and J. M. Rosen. An interactive graphics-based model of the lower extremity to study orthopaedic surgical procedures. *IEEE Trans. Biomed. Eng.* 37:757–767, 1990.
- ¹¹Demers, M. S., S. Pal, and S. L. Delp. Changes in tibiofemoral forces due to variations in muscle activity during walking. *J. Orthop. Res.* 32:769–776, 2014.
- ¹²Franz, J. R., and R. Kram. Advanced age and the mechanics of uphill walking: a joint-level, inverse dynamic analysis. *Gait & Posture*. 39:135–140, 2014.
 - ¹³Friederich, J. A., and R. A. Brand. Muscle fiber architecture in the human lower limb. *J. Biomech.* 23:91–95, 1990.
- ¹⁴Galle, S., P. Malcolm, W. Derave, and D. De Clercq. Adaptation to walking with an exoskeleton that assists ankle extension. *Gait & Posture*. 38:495–499, 2013.
- ¹⁵Griffin, T. M., and F. Guilak. The role of mechanical loading in the onset and progression of osteoarthritis. *Exerc. Sport Sci. Rev.* 33(4):195–200, 2005.
- ¹⁶Haight, D. J., Z. F. Lerner, W. J. Board, and R. C. Browning. A comparison of slow, uphill and fast, level walking on lower extremity biomechanics and tibiofemoral joint loading in obese and nonobese adults. *J. Orthop. Res.* 32:324–330, 2014.
- ¹⁷Hall, M., L. Diamond, G. Lenton, C. Pizzolato, and D. Saxby. Immediate effects of valgus knee bracing on tibiofemoral contact forces and knee muscle forces. *Gait & Posture*. 68:55–62, 2018.
- ¹⁸Huang, L., J. Zhuang, and Y. Zhang. The application of computer musculoskeletal modeling and simulation to investigate compressive tibiofemoral force and muscle functions in obese children. *Comput. Math. Methods Med.* 2013. https://doi.org/10.1155/2013/305434.
- ¹⁹Kang, I., H. Hsu, and A. Young. The effect of hip assistance levels on human energetic cost using robotic hip exoskeletons. *IEEE Robot. Autom. Lett.* 4:430–437, 2019.
- ²⁰Krishnaswamy, P., E. N. Brown, and H. M. Herr. Human leg model predicts ankle muscle-tendon morphology, state, roles and energetics in walking. *PLoS Comput. Biol.* 7:e1001107, 2011.
- ²¹Kutzner, I., B. Heinlein, F. Graichen, A. Bender, A. Rohlmann, A. Halder, A. Beier, and G. Bergmann. Loading of the knee joint during activities of daily living measured in vivo in five subjects. *J. Biomech.* 43:2164–2173, 2010.
- ²²Lee, D., E. C. Kwak, B. J. McLain, I. Kang, and A. J. Young. Effects of assistance during early stance phase using a robotic knee orthosis on energetics, muscle activity, and joint mechanics during incline and decline walking. *IEEE Trans. Neural Syst. Rehabil. Eng.* 28:914–923, 2020.
- ²³Lee, D., B. J. Mclain, I. Kang, and A. Young. Biomechanical comparison of assistance strategies using a bilateral robotic knee exoskeleton. *IEEE Trans. Biomed. Eng.* 68(9):2870–9, 2021.
- ²⁴Lenton, G. K., P. J. Bishop, D. J. Saxby, T. L. A. Doyle, C. Pizzolato, D. Billing, and D. G. Lloyd. Tibiofemoral joint contact forces increase with load magnitude and walking

- speed but remain almost unchanged with different types of carried load. *PLoS ONE*. 13:e0206859, 2018.
- ²⁵Lichtwark, G. A., and A. M. Wilson. Interactions between the human gastrocnemius muscle and the Achilles tendon during incline, level and decline locomotion. *J. Exp. Biol.* 209:4379, 2006.
- ²⁶Lloyd, D. G., and T. F. Besier. An EMG-driven musculoskeletal model to estimate muscle forces and knee joint moments in vivo. *J. Biomech.* 36:765–776, 2003.
- ²⁷Mandl, L. A. Osteoarthritis year in review 2018: clinical. Osteoarthr. Cartil. 27:359–364, 2019.
- ²⁸Molinaro, D. D., A. S. King, and A. J. Young. Biomechanical analysis of common solid waste collection throwing techniques using OpenSim and an EMG-assisted solver. *J. Biomech.* 104:109704, 2020.
- ²⁹National Center for Health Statistics and National Health and Nutrition Examination Survey. *Anthropometric reference data for children and adults; United States, 2011-2014.* Hyattsville, MD: U.S. Department of Health and Human Services, Centers for Disease Control and Prevention, National Center for Health Statistics, 2016.
- ³⁰Neptune, R., and K. Sasaki. Ankle plantar flexor force production is an important determinant of the preferred walk-to-run transition speed. *J. Exp. Biol.* 208:799–808, 2005.
- ³¹Nisell, R., G. Nemeth, and H. Ohlsen. Joint forces in extension of the knee: analysis of a mechanical model. *Acta Orthop. Scand.* 57:41–46, 1986.
- ³²Park, E., T. Akbas, A. Eckert-Erdheim, L. Sloot, R. Nuckols, D. Orzel, L. Schumm, T. Ellis, L. Awad, and C. Walsh. A hinge-free, non-restrictive, lightweight tethered exosuit for knee extension assistance during walking. *IEEE Trans. Med. Robot. Bionics*. 2(2):165–175, 2020.
- ³³Pizzolato, C., D. G. Lloyd, M. Sartori, E. Ceseracciu, T. F. Besier, B. J. Fregly, and M. Reggiani. CEINMS: a toolbox to investigate the influence of different neural control solutions on the prediction of muscle excitation and joint moments during dynamic motor tasks. *J. Biomech.* 48:3929–3936, 2015.
- ³⁴Sartori, M., D. Farina, and D. G. Lloyd. Hybrid neuro-musculoskeletal modeling to best track joint moments using a balance between muscle excitations derived from electromyograms and optimization. *J. Biomech.* 47:3613–3621, 2014.
- ³⁵Sasaki, K., and R. R. Neptune. Individual muscle contributions to the axial knee joint contact force during normal walking. *J. Biomech.* 43:2780–2784, 2010.
- ³⁶Scherpereel, K. L., N. B. Bolus, H. K. Jeong, O. T. Inan, and A. J. Young. Estimating knee joint load using acoustic emissions during ambulation. *Ann. Biomed. Eng.* 49(3):1000–1011, 2020. https://doi.org/10.1007/s10439-020-02641-7.
- ³⁷Schutte, L. M. Using Musculoskeletal Models to Explore Strategies for Improving Performance in Electrical Stimulation-Induced Leg Cycle Ergometry. Ann Arbor: Stanford University, p. 192, 1993.
- ³⁸Starkey, S. C., G. K. Lenton, D. J. Saxby, R. S. Hinman, K. L. Bennell, T. Wrigley, D. Lloyd, and M. Hall. Effect of exercise on knee joint contact forces in people following medial partial meniscectomy: a secondary analysis of a randomised controlled trial. *Gait & Posture*. 79:203–209, 2020.



- ³⁹Steele, K. M., M. S. DeMers, M. H. Schwartz, and S. L. Delp. Compressive tibiofemoral force during crouch gait. *Gait & Posture*. 35:556–560, 2012.
- ⁴⁰Taylor, W. R., M. O. Heller, G. Bergmann, and G. N. Duda. Tibio-femoral loading during human gait and stair climbing. *J. Orthop. Res.* 22:625–632, 2004.
- climbing. *J. Orthop. Res.* 22:625–632, 2004.

 ⁴¹Wickiewicz, T. L., R. R. Roy, P. L. Powell, and V. R. Edgerton. Muscle architecture of the human lower limb. *Clin Orthop Relat Res.* 179:275–283, 1983.
- ⁴²Yamaguchi, G. T., and F. E. Zajac. A planar model of the knee joint to characterize the knee extensor mechanism. *J. Biomech.* 22:1–10, 1989.

Publisher's Note Springer Nature remains neutral with regard to jurisdictional claims in published maps and institutional affiliations.

